UDC 541.136 doi: 10.33609/0041-6045.85.10.2019.67–77

Yu.V. Shmatok[1], N.I. Globa[1*], V.M. Nikitenko[2], E.A. Babenkov[2], V.S. Kublanovsky[2]

ELECTROCHEMICAL CHARACTERISTICS OF TIN FILMS IN CYCLING IN LITHIUM-ION BATTERIES **

[1] *Joint Department of Electrochemical Energy Systems of National Academy of Sciences of Ukraine, 38a Vernadsky boulevard, Kyiv, 03680, Ukraine*
[2] *V.I. Vernadsky Institute of General and Inorganic Chemistry of National Academy of Sciences of Ukraine, 32/34 Academic Palladin Avenue, Kyiv, 03142, Ukraine*
[*] *e-mail: gnl-n@ukr.net*

Thin electrolytic fine tin sediments were obtained from pyrophosphate electrolyte under different electrolysis conditions and duration. The electrochemical characteristics of tin coatings as anode materials of lithium-ion batteries are studied using potentiodynamic and galvanostatic cycling methods. The effect of the properties of coatings, in particular their mass, on the value of specific capacitance and its stability, including during discharge with different current densities, has been established. It is shown that the studied tin sediments have high initial specific capacity that is close to theoretically possible. The maximum stability of the specific capacity during cycling is characteristic of electrodes with minimal masses of precipitation. The impedance spectra recorded for the studied electrodes in the initial state and after the first lithiation are analyzed.

K e y w o r d s: electrodeposition, pyrophosphate electrolyte, tin films, specific capacity, reversibility, lithium-ion battery.

INTRODUCTION. In modern lithium-ion batteries (LIB), graphite is most widely used as anode. It is capable of providing more than a thousand charge/discharge cycles with a relatively low capacity loss. However, carbon anodes do not meet a number of requirements for modern LIBs, since they have a low specific capacity (372 $mA \cdot h \cdot g^{-1}$), a low discharge rate, and a relatively narrow operating temperature range [1]. The development of new anode materials, characterized by high specific capacitances and density of discharge currents, is an urgent task. Alloy-forming materials are considered as an alternative to replacing carbon anodes, among which the most promising are silicon, tin, and tin-containing composite coatings, in particular alloys of tin with nickel, cobalt, copper, zinc, antimony [2, 3].

The authors of [4, 5] proposed methods for increasing the specific characteristics of carbon materials when used in LIB by producing thin films of Sn/C nanocomposites on the carbon surface or by dispersing tin into an electrically

** This work was carried out in the framework of the target research program of the National Academy of Sciences of Ukraine ‘‘New Functional Substances and Materials of Chemical Engineering”, project No. 7–19, 2019.

conductive microporous carbon membrane.

One of the simplest and most easily controlled methods for producing coatings with metals and alloys, which makes possible to control their structure and functional properties, is electrochemical deposition of complex electrolytes from aqueous solutions [6, 7].

The morphology, structure, and, consequently, the properties of the resulting coatings are affected by the electrolysis parameters and the electrolyte composition, in particular, the composition of electrochemically active complexes (EAC) directly discharged on the electrode [8, 9]. The authors of [10–12] substantiated the criteria for the selection of ligands for complex, including multiligand, electrolytes and the conditions for their compatibility in one coordination sphere during the formation of mixed-ligand complex compounds. This allows one to control the braking of the electrode process and, therefore, the structure and functional properties of the resulting coatings [12, 13].

Earlier [14], we published the results of studies of thin tin films obtained from complex tartrate (KNatart), citrate (Na_3citr), and citrate-trilonate (Na_3citr/Na_2H_2edta) electrolytes as LIB anodes. It has been shown that the nature of the ligand determines such electrochemical characteristics as the specific capacitance value and cycling efficiency. The most stable charge/discharge characteristics were obtained for tin sediments deposited from citrate electrolyte [14].

Of scientific interest is the study of electrochemical properties (specific capacity, corrosion resistance, and cycling efficiency in LIB) of thin tin deposits obtained from pyrophosphate electrolyte under various electrolysis conditions, as one of the most promising anode materials for LIB.

The process of electrodeposition of tin(II) from a pyrophosphate electrolyte, unlike tartrate, citrate, and citrate-trilonate electrolytes, is limited by the previous chemical reaction of dissociation of the complexes $[Sn(HP_2O_7)(P_2O_7)]^{5-}$ or $Sn(P_2O_7)_2]^{6-}$, composition of which is determined by pH [10]. This allows to control the breaking of the electrode process and, therefore, the morphology, structure and properties of the obtained tin films, in particular their porosity. In addition, pyrophosphate electrolytes are economically more advantageous than, for example, citrate or tartrate electrolytes.

In this regard, this work is devoted to the study of the electrochemical properties of thin tin deposits obtained from pyrophosphate electrolyte under different electrolysis conditions.

EXPERIMENT AND DISCUSSION OF THE RESULTS. Tin precipitates were obtained on a copper foil substrate with a surface of 2 cm^2 from a pyrophosphate electrolyte of the composition, $g \cdot l^{-1}$: $SnCl_2 \cdot 2H_2O$ – 90, $K_4P_2O_7 \cdot 3H_2O$ – 425, NH_4Cl – 50, at pH 7.2. Electrolysis was carried out at current densities of 1–1.5 mA cm^{-2} and temperature of 25 °C for 15–45 min. Platinum was used as the anode. For the preparation of electrolytes, reagents of the analytical grade were used.

Before applying precipitation, the surface of the copper substrate was degreased with soda and Viennese lime, etched and activated according to the procedure [15], washed with distilled water and dried at a temperature of 60 °C. The electrolysis parameters were set using a PI-50-1 potentiostat and a PR-8 programmer. The electrolysis was carried out under conditions of natural convection. The mass of tin precipitation was determined on an analytical balance "ADV-200M" with an accuracy of ±0.01 mg.

Electrochemical studies of the obtained tin precipitates were carried out in disk cells of size 2016. A 1M solution of lithium *bis*-(tri-fluoromethane) sulfonimide (LiTFSI) in a mixture of fluoroethylene carbonate and dimethyl carbonate solvents taken in a mass ratio of 1:3 was used as an electrolyte. As an auxiliary electrode and a reference electrode lithium metal was used. Celgard 2400 polypropylene film with thickness of

25 μm was used as a separator. Working electrodes with tin precipitates (S = 2 cm^2) immediately before assembling the cells were dried in vacuum at a temperature of 100 °C. All operations related to the preparation of electrodes, electrolytes and cell assembly were carried out in dry glove boxes.

Current-voltage characteristics were recorded on potentiostat P-30 ”Elins” at a sweep speed of 0.5 $mV \cdot s^{-1}$, a temperature of 25 ± 2 °C, and a voltage range of 0.01–1.20 V. For galvanostatic tests Neware Battery Testing System was used with the appropriate soft-ware. The cycling was carried out in the voltage range of 0.01–1.1 V at currents from 100 to 500 $\mu A \cdot cm^{-2}$.

The impedance curves of the two electrodes cells with tin and lithium electrodes in initial state and fully discharged (after the first lithiation) state were obtained at the frequency range from 0.08 Hz to 50 kHz and amplitude of applied voltage of 10 mV. The experiment was carried out after establishing a constant value of the open circle voltage (OCV) in the cells.

The process of incorporation of lithium into tin proceeds according to the mechanism of alloy formation and is characterized by multistage processes [16]. The maximum specific capacity of the tin electrode in the interaction with lithium is 994 $mA \cdot h \cdot g^{-1}$, which corresponds to the formation of an alloy of the composition $Li_{4.4}Sn$. The mass of tin precipitation obtained from pyrophosphate electrolyte, and the electrolysis parameters are presented in table 1.

A typical cyclic current–voltage curve of a tin electrode obtained at a sweep speed of 0.5 $mV \cdot s^{-1}$ is shown in fig. 1. There are several cathode and anode peaks on the curve. The cathode peak in the potential region of 0.68 V is associated with the formation of a solid electrolyte interface (SEI) on the tin surface [17], the formation of which prevents further decomposition of the electrolyte. A large peak at a potential of ~ 0.3 V corresponds to the formation of

T a b l e 1

Parameters of electrolysis and mass of tin precipitation obtained from pyrophosphate electrolyte

Sample	Electrolysis duration, min	Current density, $mA \cdot cm^{-2}$	Mass of precipitate, $mg \cdot cm^{-2}$	Current efficiency, %
1	15	1.0	0.25	44.7
2	15	1.5	0.27	33.0
3	30	1.0	0.51	45.7
4	30	1.5	0.53	31.8
5	45	1.0	0.78	46,7
6	45	1.5	0.87	34.8

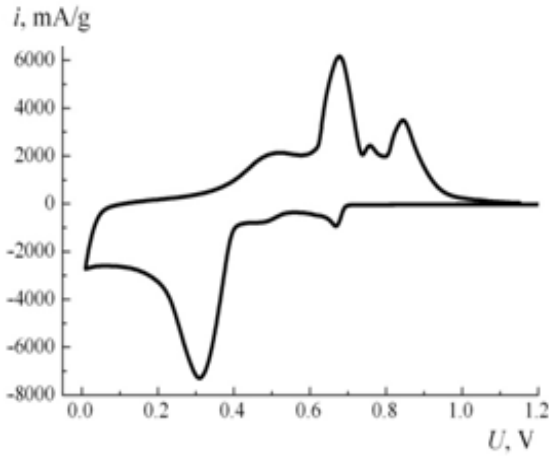

Fig. 1. Typical current-voltage curve of a tin electrode at the potential sweep rate of 0.5 $mV \cdot s^{-1}$.

analloy of lithium with tin. Peaks on the anode branch of the current–voltage curve at potentials of 0.68, 0.75, and 0.84V are associated with the reverse process, which is characterized by the formation of intermetallic compounds of different phase composition [18].

The galvanostatic charge/discharge curves of Sn electrodes with a mass of 0.25–0.87 $mg \cdot cm^{-2}$, obtained in the first cycle, are shown in fig. 2. For efficient cycling, the range of charge/discharge voltages, in accordance with the voltammetry data, was set in the range from 0.01 to

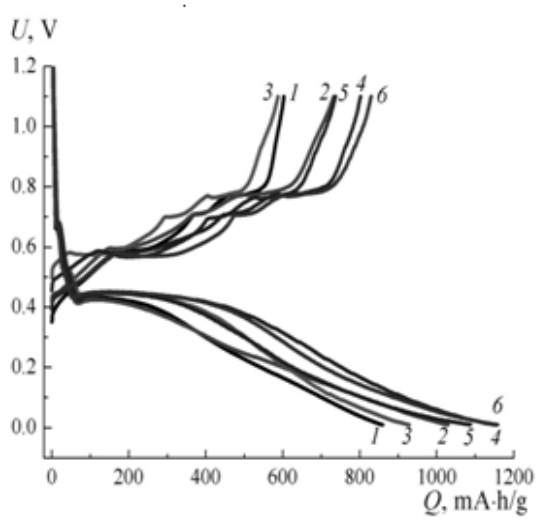

Fig. 2. Discharge/charge curves of the first cycle at the cycling current density of 100 μA·cm^{-2} for Sn-electrodes. The numbers on the curves correspond to the numbers of the samples in table 1 (the same is presented in fig. 4,5).

1.1 V. This allows to reduce the ireversible loss of capacity during the introduce-tion/extraction of lithium, which occurs at a vol-tage above 1.5 V [19]. According to published data [20], fusion of lithium with tin proceeds with the formation of seven intermediate phases, the theoretically calculated potentials of which, depending on the phase composition, are in the range of 0.76–0.38 V. However, the real potentials corresponding to phase transitions are determined not only by thermodynamics, but also by kinetic constaints, depending on the conditions for obtaining precipitation and the conditions of the cathodic process. The voltage of the site on the presented cathode curves corresponds to 0.4–0.45 V, and its length is in the range from ~200 to ~500 mA·h·g^{-1} and depends on the weight of the precipitate and electrolysis conditions. The further process of alloy formation is characterized by a gentle curve. The anode curves are more complex and have several kinks at voltages of 0.58, 0.71 and 0.78 V, which are close in magnitude to the potentials of the anode process (fig. 1).

The corresponding values of the specific capacities of the discharge and charge, as well as the coulombic efficiency in the first cycle for the studied electrodes are presented in table 2. The obtained values of the discharge specific capacity are in the range of 860–1158 mA·h·g^{-1}, and their analysis indicates an increase in specific capacity with increasing mass of sediment. Corresponding charging capacities range from 602 to 830 mA·h·g^{-1}. The relatively low value of coulombic efficiency (63–72 %) in the first cycle of lithium incorporation and extraction is associated with side processes caused by the formation of SEI and the decomposition of electrolyte [5]. However, already from the second cycle, the coulombic efficiency increases to 90 %.

Table 2

Specific capacities and coulombic efficiency of Sn-electrodes at the first cycle

Sample	$Q_{discharge}$ *	Q_{charge} *	Coulombic efficiency, %
	mA·h·g^{-1}		
1	860	602	70
2	1029	733	71
3	928	588	63
4	1151	802	70
5	1087	737	68
6	1158	830	72

* Q, mA·h·g^{-1} — specific capacity of tin films on the first cycle.

Fig. 3 shows the dependence of the specific capacity of tin precipitates obtained at electrolysis currents of 1.0 and 1.5 mA·cm^{-2} during the first lithiation on their mass. The obtained dependences in both cases are not linear, which implies a decrease in the utilization coefficient of the tin precipitate when a certain mass (thickness) is reached at different cyclic current densities.

The results of galvanostatic cycling of tin electrodes (samples 1–4) at differen t discharge current densities are presented in fig. 4. The minimum loss of specific capacity both within one

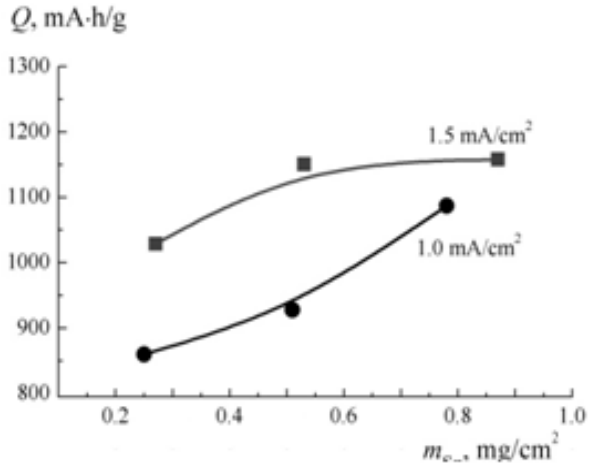

Fig. 3. Dependences of the specific discharge capacity at the first lithiation on the mass of tin precipitation.

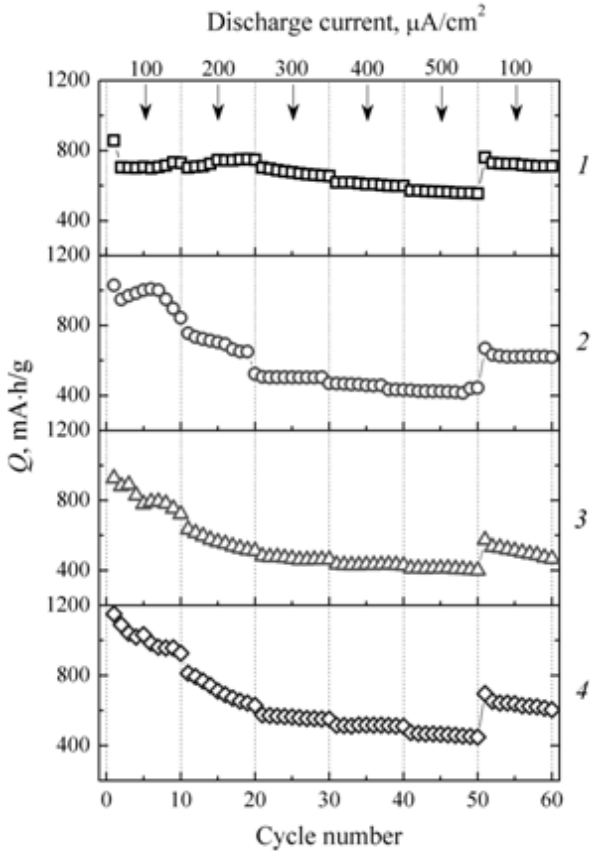

Fig. 4. Cycling performance of Sn-electrodes at different discharge currents (charge current – 100 μA·cm^{-2}).

discharge current and with its increase from 100 to 500 μA·cm^{-2} was obtained for sample 1, which is characterized by a minimum sediment mass of 0.25 mg·cm^{-2}. Sample 2 with almost the same mass of the tin film (0.27 mg/cm^2), as follows from fig. 4, is characterized by a significantly larger loss of specific capacity during prolonged cycling. This is apparently due to the different morphology, structure and properties of tin films, primarily their porosity, obtained at two different polarizing current densities. With increasing deposition current density (sample 2), the porosity of the tin film and its stability during long-term cycling decrease. For the remaining samples, an increase in the rate of decrease in specific capacity with an increase in the mass of precipitation is observed. At the same time, in all cases, at later stages of cycling, relative stabilization of the specific capacity is observed, which after the 60 cycles is in the range from 470 to 710 mA·h·g^{-1}. The corresponding discharge/charge curves of the final cycles are presented in fig. 5.

The profile of charge/discharge curves changes significantly in comparison with the curves of the first cycle (fig.2). The kinks observed on

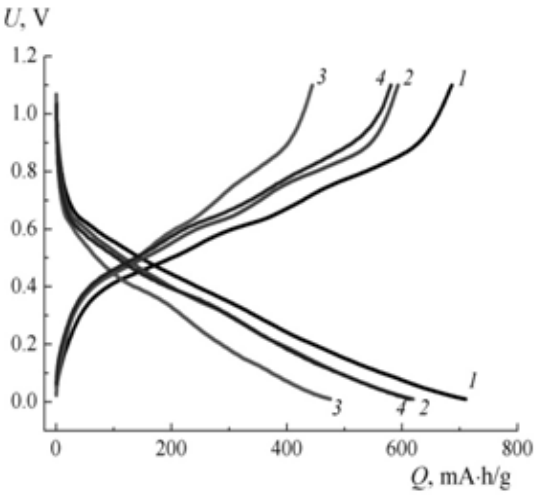

Fig. 5. Discharge/charge curves of the 60th cycle at the cycling current density of 100 μA·cm^{-2} for Sn-electrodes.

the corresponding curves of the first cycle at the end of the cycle are smoothed. These differences are associated with a change in the structure of tin deposits and the release of the electrode to a more stable cycling mode. This is confirmed by a decrease in capacity loss during cycling in later charge/discharge cycles.

Comparison of the obtained results with the data of [14] indicates that the specific capacity of tin films obtained from pyrophosphate electrolyte is significantly higher compared to the capacity of tin films obtained from citrate-trilonate (750 $mA \cdot h \cdot g^{-1}$), citrate (500 $mA \cdot h \cdot g^{-1}$) and tartrate (400 $mA \cdot h \cdot g^{-1}$) electrolytes. Higher specific characteristics of tin precipitation during lithium incorporation and extraction may be due to the difference in the mechanism of their electrolytic production. The process of electrodeposition of tin (II) from a pyrophosphate electrolyte is limited by the previous chemical reaction of dissociation of the unprotonated complex $[Sn(P_2O_7)_2]^{6-}$ [10]:

$$[Sn(P_2O_7)_2]^{6-} \leftrightarrow [SnP_2O_7]^{2-} + P_2O_7^{4-},$$

that allows you to control the morphology, structure and quality of the obtained tin sediments, especially their thickness and porosity.

The influence of electrolysis conditions on the effective resistance of tin electrodes is determined. For studies, we used cells with the initial (unlithiated) Sn electrodes and cells after the first cycle of lithium intercalation (lithiation) to a voltage of 0.01 V.

The impedance spectra of the original cells in the Nyquist coordinates Z´ – Z´´, where Z´ and Z´´ are the real and imaginary components of the impedance, respectively, are shown in fig. 6, *a*. The presented curves are characterized by two sections: the first is in the high-frequency region (from 50 kHz to 1 Hz), and the second in the frequency range from 1 to 0.08 Hz. The initial resistance value obtained by extrapolating the hodograph to the real Z´ axis at a frequency of 50 kHz is responsible for the resistance of the

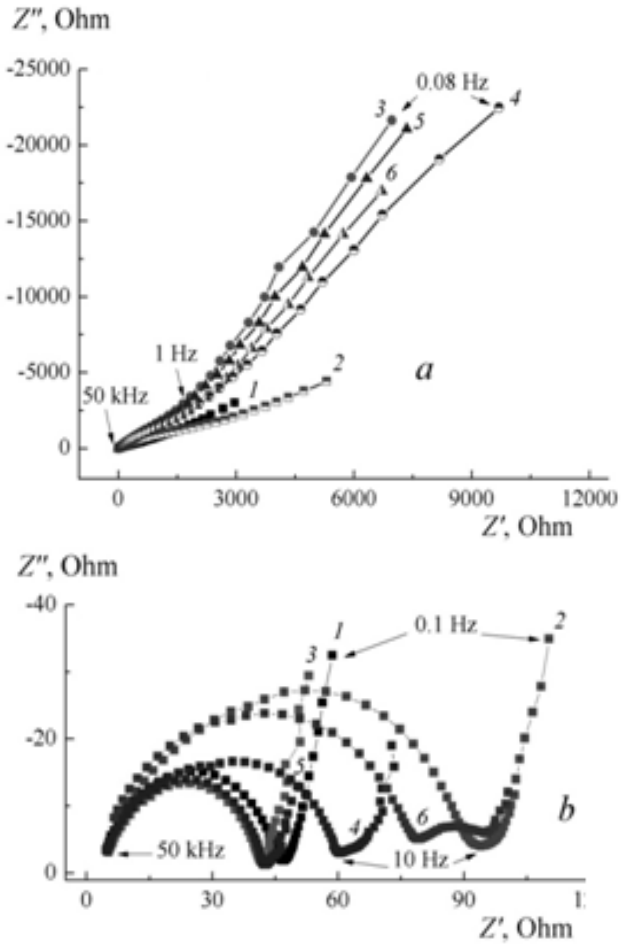

Fig. 6. Impedance spectra of the Li–Sn system in Nyquist coordinates before cycling (*a*) and after the first discharge (*b*).

electrolyte layer (Rel) in the interelectrode space and the separator. The value of this resistance for all the studied electrodes is quite close and is about 2 Ohm. Using the well-known equation $k = l/S \cdot R$, where k is the conductivity, l is the thickness of the electrolyte layer (corresponds to the thickness of the separator $–2.5 \cdot 10^{-3}$ cm), S is the electrode surface (2 cm^2), and $R = R_{el}$, the conductivity of the electrolyte layer was calculated, which is $\sim 0{,}6 \cdot 10^{-3}$ $mS \cdot cm^{-1}$, which is close to the conductivity of the electrolyte in the layer of the Celgard 2400 separator [21].

The dependences obtained in the high-

frequency region can be considered as a curve in the form of an incomplete arc. At low frequencies, this curve turns into a straight line with tilt angles of 48° and 41°, respectively, for precipitation with a tin mass of 0.25 and 0.27 mg cm^{-2} (curves *1* and *2*). This tilt angle may be due to the presence of slight diffusion limitations. An increase in the mass of tin sediment leads to an increase in tilt angles that are 69–73°, which indicates the presence of polarization phenomena associated with the accumulation or adsorption of charged particles on the surface of the electrode. This type of impedance curve is characteristic for ionistors in which the main electrochemical processes occur due to adsorption-desorption of charged particles and the absence of Faraday processes [21]. It should be noted that the source electrodes have sufficiently large resistances, which reaches several thousand Ohm. This can be caused by the presence of an oxide film formed on the surface of tin sediments after their obtaining, dry ing and storage.

The impedance spectra of electrochemical cells after the first cycle of lithiation of Sn-electrodes are significantly different from the initial ones, both in nature and in the resistance of the active and reactive parts of the impedance curve (fig.6, *b*). They consist of semicircles capturing a high frequency region, turning into samples 4 and 6, the impedance curves in the low frequ-

T a b l e 3

Resistance of the active and reactive parts of the impedance of the studied electrolytic precipitations of tin

Sample	Initial sample (OCV-2.2 V)			Sample after 1st discharge to 0.01 V*		
	f, Hz	Z′, Ω	–Z′′, Ω	*f*, Hz	Z′, Ω	–Z′′, Ω
1	50 000	2.23	3.14	50 000	8.48	2.65
	1	1053	793	10	47.17	1.891
	0.08	2965	3000	0.1	58.6	32.42
2	50 000	4.87	4.39	50 000	9.47	9.48
	1	2068	1485	10	94	4
	0.08	5305	4419	0.1	110	34.9
3	50 000	2.3	1.55	50 000	5.21	3.1
	1	1645	2920	10	42.4	1.71
	0.08	6963	21640	0.1	50.64	24.38
4	50 000	2.32	1.91	50 000	7.5	7.72
	1	2314	3433	10	61.36	3.15
	0.08	9691	22500	0.1	73.4	15.86
5	50 000	2.29	7.7	50 000	4.94	3.56
	1	1763	2960	10	42.6	1.28
	0.08	7344	21080	0.1	48.96	10.7
6	50 000	2.31	1.88	50 000	6.65	8.24
	1	1798	2472	10	82.8	6.09
	0.08	6702	17000	0.1	100	12.04

* The values of OCV of discharged cells: 1 – 0.315 V, 2 – 0.347 , 3 – 0.487 , 4 – 0.441 , 5 – 0.396, 6 – 0.391 V.

ency region have an additional section in the form of a small semicircle. The semicircle in the high-frequency region is characteristic for many lithium systems in which a passive film is formed on the lithium electrode, the nature and character of which depend on the composition of the electrolyte and the state of the electrodes [22, 23].

Such character of the impedance spectra, according to the authors of [24], allows to separate the stages of electrochemical processes, the first of which corresponds to the transfer of lithium cations across the electrode/electrolyte interface taking into account the formed SEI, and the second stage of the process is the diffusion of lithium incorporated into the Li_xSn alloy. The presence of a second semicircle in the impedance curves for electrodes with maximum tin deposit mass indicates the formation of an additional solid electrolyte layer on their surface. As a result, the resistance of such electrodes increases in both the high and low frequencies. The angle of inclination of the straight line at low frequencies is greater than 45°. The authors of [25], who studied the impedance spectroscopy of thin tin deposits during the incorporation and extraction of lithium, showed that an inclination angle of 45°, corresponding to the limiting stage of diffusion, is characteristic only at a voltage of 0.65 V. At more positive potentials, other processes including the accumulation of charge, which causes the deviation of the slope of the curve in the low-frequency region from 45°, limit lithium diffusion in the tin structure.

Table 3 shows the values of the resistances Z′ and Z′′ depending on the frequency for the studied Sn electrodes. The electrodes obtained at a current density of 1 $mA \cdot cm^{-2}$ (1, 3, 5) are characterized by lower resistance of the active part of the impedance than the electrodes obtained at a current density of 1.5 $mA \cdot cm^{-2}$, with almost the same mass of tin precipitation. All the studied electrodes after the first lithiation cycle are characterized by an increase in resistance at a frequency of 50 kHz, which may be due to a change in the porosity and thickness of the deposit because of the introduction of lithium. This is in good agreement with the fact that with the introduction of lithium into tin and the formation of the $Li_{4.4}Sn$ alloy its volume increases to ~ 300 % [26].

CONCLUSIONS. Thin electrolytic fine sediments were obtained from pyrophosphate electrolyte under different electrolysis conditions and its duration. Electrochemical tests of the obtained tin deposits as the anode material for LIB showed that the samples under study have a high initial specific capacity ranging from 860 to 1158 $mAh \cdot g^{-1}$ and are characterized by different stability during long-term cycling. Tin deposits with a minimum mass deposited at a current density of 1.0 $mA \cdot cm^{-2}$ demonstrate the best stability of the specific capacity during long-term cycling, including when discharged by different current densities. For the remaining samples, the loss in specific capacity increases with increasing mass of tin sediment.

The impedance spectra recorded for the initial Sn electrodes and after the first lithiation have different shapes and values of the corresponding resistances, which indicates differences in the passage of the main processes in a system with a tin electrode depending on the mass of the coating.

ACKNOWLEDGEMENTS. The authors are grateful to Dr.Sc. K.D. Pershina for assistance in the discussion of the results of impedance studies.

ЕЛЕКТРОХІМІЧНІ ХАРАКТЕРИСТИКИ ПЛІВОК ОЛОВА ПРИ ЦИКЛУВАННІ В ЛІТІЙ-ІОННИХ АКУМУЛЯТОРАХ

Ю.В. Шматок[1], Н.І. Глоба[1*], В.М. Нікітенко[2], Є.А. Бабенков[2], В.С. Кублановський[2]

[1]Міжвідомче відділення електрохімічної енергетики НАН України, бульвар Вернадського, 38а, Київ, 03680, Україна
[2]Інститут загальної та неорганічної хімії

ім. В.І. Вернадського НАН України, просп. Академіка Палладіна, 32/34, Київ, 03142, Україна
** e-mail: gnl-n@ukr.net*

Методами потенціодинамічного та гальваностатичного циклування в 1М фторетиленкарбонат-диметилкарбонатному розчині *біс*-(трифторметан)сульфоніміду літію (LiTFSI) в елементах дискової конструкції з габаритами 2016 досліджено електрохімічні характеристики (питома ємність, густина заряд-розрядного струму, корозійна стійкість, ефективність циклування) олов'яних покриттів як анодних матеріалів літій-іонних акумуляторів (ЛІА). Електролітичні тонкі плівки олова отримано на мідній підкладці з пірофосфатного електроліту при pH 7.2, різних режимах електролізу та його тривалості. Встановлено вплив властивостей покриттів, зокрема їх маси, на величину питомої ємності та її стабільність, у тому числі при розряді різною густиною струму. Показано, що процес інтеркаляції-деінтеркаляції літію відбувається не на поверхні електрода, а по всій товщині плівки. Досліджувані плівки олова мають високу початкову питому ємність, близьку до теоретично можливої (994 мА·ч·г$^{-1}$), і здатні без механічного руйнування забезпечувати високу густину заряд-розрядного струму. Максимальна стабільність питомої ємності при циклуванні характерна для олов'яних електродів з мінімальними масами осадів. Кулонівська ефективність Sn-електродів на першому циклі практично не залежить від товщини плівки олова і становить 70 %, надалі підвищується до 90 % . Проаналізовано спектри імпедансу, зняті для досліджуваних електродів у початковому стані та після першого циклування (літування). Спектри імпедансу, зняті для початкових Sn-електродів і після першого літування, мають різну форму та значення відповідних опорів, що вказує на відмінності в проходженні основних процесів у системі з олов'яним електродом залежно від маси покриття.

К л ю ч о в і с л о в а: електроосадження, пірофосфатні електроліти, плівки олова, питома ємність, оборотність, літій-іонний акумулятор.

ЭЛЕКТРОХИМИЧЕСКИЕ ХАРАКТЕРИСТИКИ ПЛЕНОК ОЛОВА ПРИ ЦИКЛИРОВАНИИ В ЛИТИЙ-ИОННЫХ АККУМУЛЯТОРАХ

Ю.В. Шматок[1], Н.И. Глоба[1*], В.Н. Никитенко[2], Е.А. Бабенков[2], В.С. Кублановский[2]

[1] Межведомственное отделение электрохимической энергетики НАН Украины, бульвар Вернадского, 38а, Киев, 03680, Украина
[2] Институт общей и неорганической химии им. В.И. Вернадского НАН Украины, просп. Академика Палладина, 32/34, Киев, 03142, Украина
** e-mail: gnl-n@ukr.net*

Электролитические тонкие осадки олова получены из пирофосфатного электролита при разных режимах электролиза и его длительности. Методами потенциодинамического и гальваностатического циклирования исследованы электрохимические характеристики оловянных покрытий как анодных материалов литий-ионных аккумуляторов. Установлено влияние свойств покрытий, в частности их массы, на величину удельной емкости и ее стабильность, в том числе при разряде разными плотностями тока. Показано, что исследуемые осадки олова имеют высокую начальную удельную емкость, близкую к теоретически возможной. Максимальная стабильность удельной емкости при циклировании характерна для электродов с минимальными массами осадков. Проанализированы спектры импеданса, снятые для исследуемых электродов в исходном состоянии и после первого литиирования.

К л ю ч е в ы е с л о в а: электроосаждение, пирофосфатный электролит, пленки олова, удельная емкость, обратимость, литий-ионный аккумулятор.

REFERENCES

1. Schalkwijk W.A., Scrosati B. Advanced in Lithium-ion Batteries. (New York: Plenum publishers, 2002).
2. Pridatko K.I., Churikov A.V. Anode non-carbon lithium-accumulating composite materials. *Elektrokhimicheskaya Energetica.* 2005. **5** (1): 16. [in Russian].

3. Kamali A.R., Fray D.J. Tin-based materials as advanced anode materials for lithium ion batte-ries. *Rev. Adv. Mater. Sci.* 2011. **27:** 14.

4. Maroni F., Bruni F., Suzuki N., Aihara Tu., Croce F. Electrospun tin-carbon nanocomposits as anode material for all solid state lithium-ion batteries. *J. Solid State Electrochem.* 2019. **23:** 1697.

5. Zhao H., Jiang C., He X., Ren J. Advanced structures in electrodeposited tin base anodes for lithium ion batteries. *Electrochim. Acta.* 2007. **52:** 7820.

6. Hadsoun J., Pacero S., Scrosati B. Electrodepo-sited Ni-Sn intermetallic electrodes for advan- ced lithium ion batteries. *J. Power Sources.* 2006. **160:** 1336.

7. Huang L., Wei H.B., Ke F.S., Fan X.Y., Li J.T., Sun S.G. Electrodeposition and lithium storage performance of three-demension porous reticular Sn-Ni alloy electrodes. *Electrochem. Acta.* 2009. **54:** 2693.

8. Bersirova O., Kublanovskii V. Crystalline Roughness as a Morphological Characteristic of the Surface of Electroplated Silver Coatings. *Russ. J. Appl. Chem.* 2009. **82:** 1944.

9. Bersirova O., Kublanovsky V., Cesiulis H. Electrochemical Formation of Functional Silver Coatings: Nanostructural Peculiarities. *ECS Transactions*. 2013. **50:** 155.

10. Orekhova V.V., Andryushchenko F.K. Issledovanie kineticheskih zakonomernostei electrod-nyh reakcii v poliligandnyh electrolitah. *Electrohimiya*. 1974. **10** (3): 363. [in Russian].

11. Orekhova V.V., Andryushchenko F.K. *Polyli-gand electrolytes plating*. (Kharkov: Vishcha shkola, 1979). [in Russian].

12. Kublanovsky V.S., Nikitenko V.N. Mechanism of the electrodeposition of palladium coatings from glycinate electrolytes. *J. Electroanal. Chem.* 2013. **699:** 14.

13. Kublanovsky V.S., Nikitenko V.N. Electrochemical properties of palladium(II) *trans*- and *cis*-diglycinate complexes. *Electrochim. Acta.* 2011. **56:** 2110.

14. Kublanovsky V.S., Nikitenko V.N., Globa N.I. Effect of the nature of a ligand on electrochemical characteristic of tin films in cycling in lithium-ion batteries. *Russ. J. Appl. Chem.* 2015. **88:** 407.

15. Kublanovsky V.S., Nikitenko V.N., Globa N.I. Electrochemical Deposition of Corrosion-Resistant Coatings from Tin-Nickel Alloys. *Mater. Sci.* 2017. **52:** 687.

16. Idota Y., Kubota T., Matsufuji A., Maekawa Y., Miyasaka T. Tin-based amorphous oxide: a high-capacity lithium-ion-storage material. Science. 1997. **276:** 1395.

17. Aifantis K.E., Hackney S.A., Dempsey J.P. Design criteria for nanostructured Li-ion batteries. *J. Power Sources.* 2007. **165:** 874.

18. Amadei I., Panero S., Scrosati B., Cocco G. Schif-fini L. The Ni_3Sn_4 intermetallic as novel electro-de in lithium cells. *J. Power Sources*. 2005. **143:** 227.

19. Beattie S.D., Hatchard T., Bonakdarpour A., Hewitt K.C., Dahn J.R. Anomalous, high-voltage irreversible capacity in tin electrodes for lithium batteries. *J. Electrochem. Soc.* 2003. **150:** A701.

20. Winter M., Besenhard J.O. Electrochemical lithiation of tin and tin-based intermetallics and composites. *Electrochim. Acta.* 1999. **45:** 31.

21. Globa N.I., Shmatok Y.V., Milovanova O.I., Sirosh V.A., Kirillov S.A. Electrolytic Double-Layer Supercapacitors Based on Sodium-Ion Sy-stems, with Activated-Carbon Electrodes. *Russ. J. Appl. Chem.* 2018. **91:** 187.

22. Churikov A.V., Nimon E.S., Lvov A.L. Impedance of Li—Sn, Li—Cd and Li—Sn—Cd alloys in propylene carbonate solution. *Electrochim. Acta.* 1997. **42:** 179.

23. Churikov A.V., Gamayunova I.M., Shirokov A.V. Ionic processes in solid-electrolyte passivating films on lithium. *J. Solid State Electrochem.* 2000. **4:** 216.

24. Churikov A.V., Pridatko K.I., Ivanishchev A.V., Ivanishcheva I.A., Gamayunova I.M., Zapsis K.V., Sycheva V.O. Impedance spectroscopy of lithium-tin film electrodes. *Russ. J. Electrochem.* 2008. **44** (5): 550.

25. Churikov A.V., Ivanishchev A.V., Ivanishcheva

I.A., Gamayunova I.M., Zapsis K.V., Sycheva V.O. Lithium intercalation into thin-film lithium-tin and lithium-carbon electrodes: an impedance spectroscopy study. *Elektrokhimi-cheskaya Energetica.* 2007. **7** (4): 169. [in Russian].

26. *Aravindan V., Lee Y.S., Madhavi S.* Research progress on negative electrodes for practical Li-ion batteries: beyond carbonaceous anodes. *Adv. Energy Mater*. 2015. **5**: 1402225.

Received 18.09.2019